THE JOURNAL OF BIOLOGICAL CHEMISTRY
Vol. 278, No. 39, Issue of September 26, pp. 37511–37519, 2003
Printed in U.S.A.

Surface-exposed Tryptophan Residues Are Essential for *O*-Acetylserine Sulfhydrylase Structure, Function, and Stability*

Received for publication, May 16, 2003, and in revised form, June 13, 2003
Published, JBC Papers in Press, June 17, 2003, DOI 10.1074/jbc.M305138200

Barbara Campanini‡§, Samanta Raboni‡§, Simona Vaccari‡, Lei Zhang¶, Paul F. Cook¶, Theodore L. Hazlett‖, Andrea Mozzarelli‡§, and Stefano Bettati§‡‡§§**

From the ‡Department of Biochemistry and Molecular Biology, the §National Institute for the Physics of Matter, and the ‡‡Department of Public Health, University of Parma, Parma 43100, Italy, the ¶Department of Chemistry and Biochemistry, University of Oklahoma, Norman, Oklahoma 73019, and the ‖Laboratory of Fluorescence Dynamics, University of Illinois, Urbana, Illinois 61801

***O*-Acetylserine sulfhydrylase is a homodimeric enzyme catalyzing the last step of cysteine biosynthesis via a Bi Bi ping-pong mechanism. The subunit is composed of two domains, each containing one tryptophan residue, Trp^{50} in the N-terminal domain and Trp^{161} in the C-terminal domain. Only Trp^{161} is highly conserved in eucaryotes and bacteria. The coenzyme pyridoxal 5′-phosphate is bound in a cleft between the two domains. The enzyme undergoes an open to closed conformational transition upon substrate binding. The effect of single Trp to Tyr mutations on *O*-acetylserine sulfhydrylase structure, function, and stability was investigated with a variety of spectroscopic techniques. The mutations do not significantly alter the enzyme secondary structure but affect the catalysis, with a predominant influence on the second half reaction. The W50Y mutation strongly affects the unfolding pathway due to the destabilization of the intersubunit interface. The W161Y mutation, occurring in the C-terminal domain, produces a reduction of the accessibility of the active site to acrylamide and stabilizes thermodynamically the N-terminal domain, a result consistent with stronger interdomain interactions.**

The biosynthesis of cysteine in bacteria and plants is accomplished by the pyridoxal 5′-phosphate (PLP)[1]-dependent enzyme *O*-acetylserine sulfhydrylase (OASS). PLP-dependent enzymes are currently classified into three functional families, depending on the mechanism of the catalyzed reaction, and into 5-fold types, depending on the structural arrangement. OASS belongs to the β-family and to the fold type II, with the overall reaction catalyzed by the enzyme being a β-replacement. Members of the β-family include, among others, the β-subunit of tryptophan synthase, cystathionine β-synthase, and threonine dehydratase. Depending on the subcellular compartment and on the growth conditions, many isoforms of OASS have been described (1, 2). In *Salmonella typhimurium*, the OASS-A isoform is responsible for the synthesis of L-cysteine from sulfide and *O*-acetylserine (OAS). Catalysis follows a Bi Bi ping-pong kinetic mechanism (2, 3) and is accompanied by large conformational changes that result in the transition from an open to a closed form of the enzyme (4, 5). The conformational changes are triggered by the hydrogen bonding of the α-carboxylate group of the substrate OAS to Asn^{69} and to other residues belonging to the "asparagine loop." The rearrangement of the side chain of Asn^{69} is transmitted to a subdomain of the N-terminal domain that rotates by 13° from the position occupied in the native enzyme. The conformational changes result in the formation of new hydrogen bonds and hydrophobic interactions between the N- and C-terminal domains. The microenvironment generated by these structural rearrangements stabilizes and orients the external aldimine for the elimination reaction and protects the highly reactive α-aminoacrylate intermediate formed upon acetate elimination.

A low thermodynamic stability was evidenced for holo-OASS (6). Most of the stabilization free energy was demonstrated to derive from the binding of the cofactor to the active site, with a more pronounced effect on the C-terminal domain (7), which appears to be more stable than the N-terminal domain. The lower stability of the N-terminal domain supports the notion of a relationship between a marginal structural stabilization and the flexibility required for catalysis.

OASS possesses two tryptophan residues: Trp^{50} in the N-terminal domain and Trp^{161} in the C-terminal domain. Both residues are exposed to solvent, with Trp^{161} located in a more hydrophilic environment than Trp^{50} (Fig. 1) (8). Upon excitation at 298 nm, an energy transfer process takes place between the tryptophans and PLP. Structural data (8) indicate that, although both tryptophans are at the right distance from PLP to transfer their excitation energy to the cofactor, only Trp^{50} is correctly oriented for an efficient process to take place. Tryptophan residues are often well conserved in protein sequences (9–12) and are associated with a wide variety of protein functions, from ligand binding (9, 13, 14) to DNA-protein interactions (12, 15, 16) and from structure stabilization (10, 17, 18) to protein-protein interactions (19, 20). Recently, it has been observed that often tryptophan residues are preferentially located in stable regions of proteins (21), and their substitution with other amino acids commonly results in the destabilization of the structure and in the modification of the folding/unfolding mechanism (see Ref. 14 and references therein) (22, 23). In this work, we prepared two single tryptophan mutants of OASS: W50Y and W161Y. The presence of a single tryptophan residue in the mutants allows separate probes of the structure and dynamics of the N- and C-terminal domains. The aim of the present work was to characterize the role of the tryptophans in the structure, function, and stability of OASS and to gain insight into the unfolding processes of the N- and C-terminal domains.

* The costs of publication of this article were defrayed in part by the payment of page charges. This article must therefore be hereby marked "*advertisement*" in accordance with 18 U.S.C. Section 1734 solely to indicate this fact.

** Supported by National Institutes of Health Grant RR03155.

§§ To whom correspondence should be addressed. Tel.: 39-0521-903721; Fax: 39-0521-903712; E-mail: stefano.bettati@unipr.it.

[1] The abbreviations used are: PLP, pyridoxal 5′-phosphate; OASS, *O*-acetylserine sulfhydrylase; OAS, *O*-acetyl-L-serine; TNB, 5-thio-2-nitrobenzoate; Ches, 2-(*N*-cyclohexylamino)ethanesulfonic acid; GdnHCl, guanidine hydrochloride; SAT, serine acetyltransferase; WT, wild type.

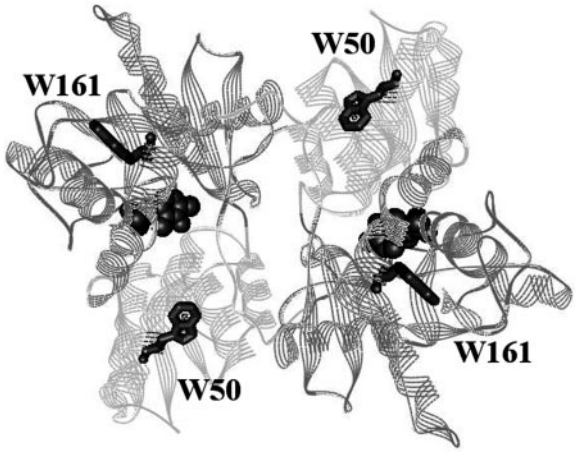

FIG. 1. **Three-dimensional structure of WT holo-OASS.** The N-terminal domain is shown in *light gray*, and the C-terminal domain is shown in *dark gray*. Trp^{50} and Trp^{161} are shown in stick mode, and PLP is shown in space-filling mode.

EXPERIMENTAL PROCEDURES

Chemicals and Molecular Biology Reagents—Hepes, *O*-acetyl-L-serine, 5,5′-dithiobis(2-nitrobenzoate), PLP, LB broth, citric acid, magnesium chloride, KH_2PO_4, $Na(NH_4)HPO_4$, thiamine, L-tryptophan, reduced glutathione, L-leucine, ampicillin, and streptomycin sulfate were from Sigma. Dithiothreitol and guanidine hydrochloride were from Fluka, and *p*-terphenyl was from Aldrich. Restriction enzymes and DNA ligase were from Amersham Biosciences, Promega, or U.S. Biochemical Corp. Oligonucleotides used for mutagenesis and sequencing were from Invitrogen or MWG-Biotech AG. All of the reagents were of the best commercially available quality and were used without further purification.

Bacterial Strains and Expression Vectors—The single tryptophan mutants were expressed in *Escherichia coli* NK3 cells that lack *cysK* and *cysM* genes. The *cysK* gene encodes for OASS-A, whereas *cysM* encodes for OASS-B (24). The plasmid pRSM40 (25) was used as the expression vector for the W50Y mutant. The plasmid pCKM3, used for the expression of the W161Y mutant, contains the *cysK* gene and its natural promoter on an *Eco*RI/*Sph*I fragment from pRSM40. The expression of *S. typhimurium* OASS-A in both pRSM40 and pCKM3 constructs is under the control of the natural promoter for *cysK*.

Site-directed Mutagenesis—The mutation $Trp^{50} \rightarrow$ Tyr was introduced using a PCR-based method with the following forward and reverse primers: 5′-GCCGTATCGGCGCCAACATGATT**TAT**GATGCCGAAAAGCG-3′ and 5′-GCAGCAACCGCGGCGCCGGAAG-3′. The sequence coding for the tyrosine residue is indicated in boldface type, and the restriction sites for the enzyme *Nar*I are underlined. WT pRSM40 was digested with *Nar*I and purified from agarose gel to generate the vector. The amplified fragment from the PCR carrying the mutation TGG → TAT was digested with *Nar*I, and the insert was purified from agarose gel and cloned into the vector.

The W161Y mutant was obtained using the kit Altered Sites® II (Promega). The mutation was introduced using the following primer: 5′-GGCCCGGAAATC**TAT**GAAGACACCGAT-3′.

The *Eco*RI/*Sph*I fragment from pRSM40 was cloned into the mutagenesis vector pALTER. *E. coli* strain ES1301 was used for plasmid propagation and plasmid isolation. *E. coli* strain JM109 was used for plasmid long term maintenance. Following mutagenesis, the *Eco*RI/*Sph*I fragment carrying the mutation was cloned into pBR322 to generate the expression vector pCKM3.

Single Tryptophan Mutants Expression and Purification—Cultures of *E. coli* NK3 transformed with mutagenized pCKM3 or pRSM40 were grown at 37 °C in a fermentor using a medium composed of Vogel Bonner E supplemented with 0.5% glucose, 5% LB, 50 μM thiamine, 40 μM L-tryptophan, 0.5 mM reduced glutathione, 50 mM L-leucine, and 100 μg/ml ampicillin. The cells were harvested by centrifugation, and the protein was partially purified by streptomycin and ammonium sulfate precipitation as described previously (26). The chromatographic procedure for the purification of the W50Y mutant was similar to that of the WT enzyme (2) and was followed by a final size exclusion chromatographic step on an Ultrogel-AcA 44 column (IBF Biotechnics). The purification of the W161Y mutant was carried out through a three-step chromatographic procedure on a HiTrap DEAE FF column (Amersham Biosciences), an Ultrogel-AcA 44 column (IBF Biotechnics), and a HiTrap Q Sepharose HP column (Amersham Biosciences). Based on SDS-PAGE, the W50Y and W161Y mutants were 99% and 90–95% pure, respectively.

Buffers—Absorbance, steady-state, and time-resolved fluorescence experiments were carried out in a buffer solution containing 100 mM Hepes, pH 7.0, in the absence and presence of defined concentrations of GdnHCl. Circular dichroism measurements were carried out in buffer solutions containing 20 mM potassium phosphate, pH 7.0, and different concentrations of GdnHCl. Denaturant-containing solutions were prepared according to Pace (27). GdnHCl concentration was determined by measuring the solution refractive index.

Absorption, Steady-state Fluorescence, and Circular Dichroism Measurements—Absorption measurements were carried out using a Cary 400 Scan or, for the activity assays, a Cary 219 spectrophotometer. Fluorescence spectra were collected on either a PerkinElmer Life Sciences LS50B or a SPEX Fluoromax-2 photon-counting fluorometer (Jobin-Yvon). Circular dichroism measurements were carried out using a JASCO J-715 spectropolarimeter. Each spectrum is the average of three measurements. Fractions of α and β structure were calculated by deconvoluting the spectra with CD Spectra Deconvolution software, version 2.1 (Gerald Böhm; see Ref. 28). Spectra were acquired at 20 ± 0.5 °C and were corrected for solvent contribution. Spectra of the single tryptophan mutants, equilibrated at different GdnHCl concentrations, were acquired after an incubation of 24 h at 20 °C.

Fluorescence Quenching Measurements—The accessibility of the cofactor of WT and W161Y OASS was assessed by fluorescence quenching with acrylamide. Acrylamide was chosen due to its neutral nature and the absence of ionic strength effects on the fluorescence properties of the cofactor. Experiments on the WT protein were performed both for the open and the closed form of the enzyme. Experiments were carried out on solutions containing 40 μM OASS and either 100 mM Hepes, pH 7.0, for the open form of the enzyme or 100 mM Ches, pH 9.0, in the presence of 100 mM L-Ser for the closed form. Spectra, collected upon excitation at 330 nm, were corrected for solvent contribution. Data were analyzed according to a modified Stern-Volmer equation (29), assuming two fluorescent and noninteracting species, where only species A is quenchable by acrylamide,

$$\frac{F_0}{F} = \frac{1 + K^A_{SV}[Q]}{(1 + K^A_{SV}[Q])(1 - f_A) + f_A} \qquad \text{(Eq. 1)}$$

where F_0 is the fluorescence intensity in the absence of the quencher, F is the fluorescence at each given quencher concentration, K^A_{SV} is the Stern-Volmer constant relative to the accessible site *A*, [Q] is the concentration of the quencher, and f_A is the fraction of initial fluorescence emitted by species A.

Time-resolved Fluorescence Measurements—Fluorescence intensity decays were measured by the phase and modulation technique (30, 31). The instrument set up was described previously (7). Tryptophan fluorescence lifetimes of the single tryptophan mutants were measured at a protomer concentration of 3.3 μM, upon excitation at 295 nm. A *p*-terphenyl solution in ethanol (1.05 ns) was used as a lifetime standard reference.

To eliminate polarization artifacts in the intensity decay, data were collected under magic angle conditions with the excitation light polarized normal to the laboratory plane, 0°, and the emission polarizer oriented at 54.7° (30). Samples were equilibrated at 20 ± 0.5 °C using a jacketed cell holder and a circulating water bath. Data were fitted to a sum of discrete exponentials (32) with lifetime τ_i and fractional intensity f_i by the Marquardt algorithm of the Globals Unlimited software (University of Illinois, Urbana, IL) (33). A short component of 1 ps was introduced to account for any Rayleigh or Raman scattering contributions (32). The fractional contribution of the short component to the total emission was always less than 3%. Frequency-independent S.E. values of 0.2° for phase data and 0.004 for modulation data were routinely applied. The χ^2 minimization was the criterion used to select the best fits (31, 32).

Equilibrium Denaturation Curves—The dependence of signal intensity I on denaturant concentration [D] was fitted to a two-state model according to the equation,

$$I = \frac{I_N + (I_U + S_U[D])e^{\frac{([D] - D_{50})m}{RT}}}{1 + e^{\frac{([D] - D_{50})m}{RT}}} \qquad \text{(Eq. 2)}$$

where I is either the fluorescence emission intensity at a given wavelength or the mean residue ellipticity at 222 nm, I_N and I_U are the extrapolated signal values for the native and denatured protein, respec-

tively, S_U is a post-transitional slope reflecting the dependence of the signal on denaturant concentration, D_{50} is the denaturant concentration at half-transition, and m is the denaturant index. The experimental data points were converted to fraction of total effect F_U by using the fitting parameters previously determined, according to the equation,

$$F_U = \frac{I_N - I}{I_N - (I_U + S_U[\mathrm{D}])} \quad \text{(Eq. 3)}$$

The equilibrium unfolding constants K_U at each denaturant concentration were calculated from the equation,

$$K_U = \frac{F_U}{1 - F_U} \quad \text{(Eq. 4)}$$

The K_U values were used to calculate the unfolding free energies.

$$\Delta G^0_U = -RT \ln K_U \quad \text{(Eq. 5)}$$

$\Delta G^0_{0,U}$, the free energy change in the absence of denaturant, and m were calculated using the linear extrapolation method (34).

$$\Delta G^0_U = \Delta G^0_{0,U} - m[\mathrm{D}] \quad \text{(Eq. 6)}$$

D_{50} was calculated as follows:

$$D_{50} = \frac{\Delta G^0_{0,\mathrm{U}}}{m} \quad \text{(Eq. 7)}$$

Reversibility of the Denaturation Reaction—The calculation of thermodynamic parameters from equilibrium denaturation curves requires that the denaturation reaction is fully reversible (27). The reversibility of the denaturation of WT holo-OASS and of W161Y and W50Y mutants was assessed diluting a solution of the unfolded enzyme in 100 mM Hepes, pH 7.0, and monitoring the kinetics of the refolding reaction via fluorescence emission spectroscopy upon excitation at 298 nm. The native emission spectrum of WT holo-OASS was recovered within 1 h. A similar result was obtained for W161Y mutant. On the contrary, the reversibility of the unfolding of the W50Y mutant appears to be only partial, since the enzyme never recovers the fluorescence emission spectrum typical of the native protein. For this reason, the fitting of the equilibrium denaturation curves of W50Y mutant only provides indicative D_{50} values, useful for comparison with the WT enzyme but devoid of any thermodynamic significance.

Enzyme Activity—A schematic mechanism for the OASS-A reaction is given in Scheme 1.

$$E \underset{k_2}{\overset{k_1\mathrm{A}}{\rightleftharpoons}} E(\mathrm{SB}_1) \underset{k_4}{\overset{k_3}{\rightleftharpoons}} E(\mathrm{AA})\mathrm{P} \xrightarrow{k_5} E(\mathrm{AA}) \underset{k_8}{\overset{k_7\mathrm{B}}{\rightleftharpoons}} E(\mathrm{AA})\mathrm{B} \underset{k_{10}}{\overset{k_9}{\rightleftharpoons}} E(\mathrm{SB}_2) \xrightarrow{k_{11}} E$$

SCHEME 1

where A, B, and P represent OAS, TNB, and acetate, respectively; E is the free enzyme, $E(\mathrm{SB}_1)$ is the OAS external Schiff base, $E(\mathrm{SB}_2)$ is the *S*-(3-carboxy-4-nitrophenyl)-L-cysteine external Schiff base, and $E(\mathrm{AA})$ is the α-aminoacrylate Schiff base. For the reported kinetic mechanism, when k_5 is fast compared with k_3 and k_4 (see also Refs. 35 and 36), the following expressions for k_{cat}, K_{OAS}, and K_{TNB} apply,

$$\frac{V}{E_t} = \frac{k_3}{1 + \left(\frac{k_3}{k_9}\right)\left(1 + \frac{k_{10}}{k_{11}}\right) + \frac{k_3}{k_{11}}} \quad \text{(Eq. 8)}$$

$$K_{\mathrm{OAS}} = K_{d(\mathrm{OAS})}\left[\frac{\left(1 + \frac{k_3}{k_2}\right)}{1 + \frac{k_3\left(1 + \frac{k_{10}}{k_{11}}\right)}{k_9} + \frac{k_3}{k_{11}}}\right] \quad \text{(Eq. 9)}$$

where $K_{d(\mathrm{OAS})} = k_2/k_1$, and

$$K_{\mathrm{TNB}} = K_{d(\mathrm{TNB})}\left[\frac{\frac{k_9}{k_8} + 1 + \frac{k_{10}}{k_{11}}}{k_9\left(\frac{1}{k_3} + \frac{1}{k_{11}}\right) + 1 + \frac{k_{10}}{k_{11}}}\right] \quad \text{(Eq. 10)}$$

where $K_{d(\mathrm{TNB})} = k_8/k_7$.

Enzyme activity was assayed using OAS and TNB as substrates in 100 mM Hepes, pH 7.0, at 20 °C (2). OAS and TNB concentrations were varied over a range of 0.5–2 mM and 25–100 μM, respectively. Since under these conditions neither substrate inhibits OASS activity, the initial velocity patterns were fitted to the equation for a simple Bi Bi ping-pong kinetic mechanism (37)

$$v = \frac{V_{\max}[\mathrm{OAS}][\mathrm{TNB}]}{K_{\mathrm{OAS}}[\mathrm{TNB}] + K_{\mathrm{TNB}}[\mathrm{OAS}] + [\mathrm{OAS}][\mathrm{TNB}]} \quad \text{(Eq. 11)}$$

Sequence Alignments—Sequences of procaryotic and eucaryotic OASS were retrieved from a nonredundant sequence data base using the BlastP program (38). Sequences were aligned using ClustalW (39, 40) with default parameters.

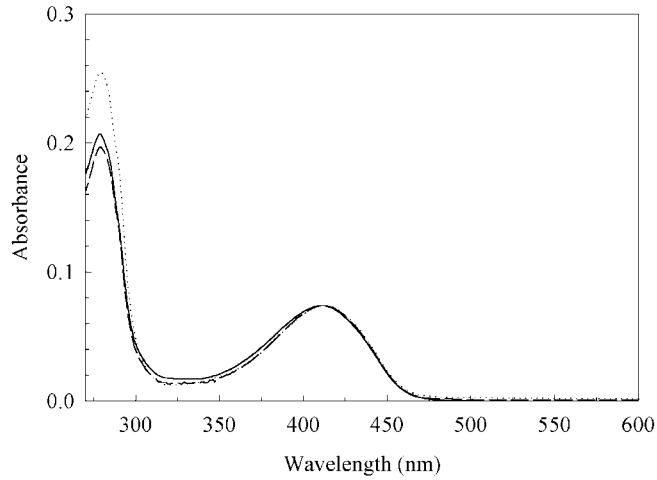

FIG. 2. **Absorption spectra of WT holo-OASS, W50Y mutant, and W161Y mutant.** Absorption spectra of W50Y OASS (*dashed line*) and W161Y OASS (*solid line*) were recorded for a solution containing 9.75 μM enzyme, 100 mM Hepes, pH 7.0, at 20 °C. The absorption spectrum of an equimolar solution of the WT enzyme is reported for comparison (*dotted line*).

RESULTS

Absorbance Spectra of W50Y and W161Y Mutants—The UV-visible spectra of the single tryptophan mutants are qualitatively similar to the spectrum of the WT protein, showing two peaks centered at 278 and 412 nm (Fig. 2). Both mutations cause a decrease of the intensity of the peak at 278 nm, due to the lower extinction coefficient of the tyrosine residue with respect to tryptophan. The peak at 412 nm, attributed to the ketoenamine tautomer of the PLP internal aldimine (3, 41, 42), is still present, indicating that the mutation has not hampered the binding of PLP to the protein active site. The ratio between the intensity at 280 nm and at 412 nm is 3.4–3.6 in WT OASS and 2.8 and 2.6 in W161Y and W50Y mutants, respectively. The spectrum of the W161Y mutant shows a slightly higher absorbance at 330 nm with respect to the WT OASS and to the W50Y mutant, suggesting the presence of an increased population of the enolimine tautomer of the internal aldimine (43).

Fluorescence Emission Spectra of Single Tryptophan Mutants—Emission spectra of the single tryptophan mutants were collected upon excitation at 298 nm (Fig. 3). The spectra are characterized by a major peak, centered at about 335 nm, due to the direct tryptophan emission, and a minor peak centered at 500 nm that, in the WT enzyme, was attributed to the energy transfer process occurring predominantly between Trp^{50} and the cofactor (8, 44). In the WT enzyme, the ratio between the tryptophans and the cofactor emissions is about 7. The peak intensity at 500 nm for the W161Y mutant and the WT protein is the same, thus reinforcing the concept of an energy transfer process that involves Trp^{50} as the principal donor. Unexpectedly, also the W50Y mutant shows a band at 500 nm, which exhibits an intensity about half of that of the wild type protein, indicating the occurrence of an energy transfer process be-

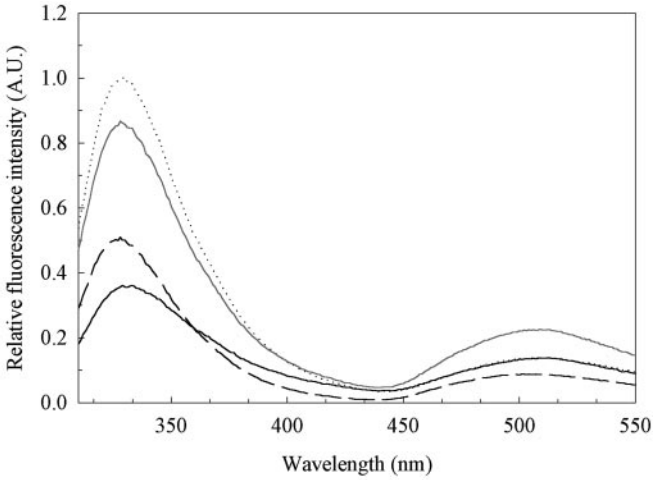

FIG. 3. **Emission spectra of WT holo-OASS, W50Y mutant, and W161Y mutant upon excitation at 298 nm.** Emission spectra of a solution containing 5 μM W50Y OASS (*dashed line*) or W161Y OASS (*solid line*), 100 mM Hepes, pH 7.0, at 20 °C were recorded upon excitation at 298 nm (excitation slit = 1 mm; emission slit = 1 mm). The emission spectrum of WT holo-OASS recorded under the same conditions is reported for comparison (*dotted line*). The sum of the fluorescence emission spectra of the W50Y and W161Y mutants is reported in *light gray*.

tween Trp^{161} and PLP. The ratio between the emission at 330 nm and the emission at 500 nm for the W161Y mutant is about 2.6, whereas the ratio increases to 5.7 for the W50Y mutant. The sum of the spectra of the two mutants gives a spectrum that is not superimposable with that of the WT enzyme (Fig. 3). In particular, the tryptophan emission intensity is lower, and the cofactor emission is about twice that measured for the wild type protein.

Fluorescence Lifetimes of W50Y and W161Y Mutants and Comparison with the WT Holo-OASS—The effect of the mutations on the local environment of the remaining tryptophan residue was examined by measuring the fluorescence emission lifetimes of the native protein (Table I). Fluorescence lifetimes are very sensitive to tryptophan microenvironment, allowing the detection of small changes in their solvent exposure. The fluorescence emission decay of WT holo-OASS is well described by three discrete species (7). The longer lifetime (5.5 ns) was mainly attributed to Trp^{50} emission, whereas the intermediate (2.1 ns) lifetime was mainly attributed to Trp^{161} emission (Table I) (7). Fluorescence emission decays of single tryptophan mutants were fitted to a sum of two exponentials plus a fixed short component (1 ps), accounting for the scattered light (Table I). The W50Y mutant is characterized by a lifetime of 2.3 ns, accounting for 91% of the total emission, and a short lifetime of about 0.8 ns. The W161Y mutant fluorescence decay is dominated by a short lifetime (0.9 ns), accounting for 75% of the emission, accompanied by a longer lifetime (4.7 ns), accounting for 25% of the emission. This finding confirms the lifetime attribution carried out on the WT enzyme (7) and indicates that the substitution of the tryptophan residue in one domain has no significant long range effects on the microenvironment of the tryptophan in the other domain.

Circular Dichroism Spectra—The circular dichroism spectra of W50Y, W161Y, and WT protein are almost coincident, indicating that the mutations have no or little effect on the secondary structure content of the protein, as shown by the deconvolution of the CD spectra with the CD Spectra Deconvolution software (28) (Table II).

Enzymatic Activity—The effect of tryptophan mutations on OASS activity was characterized using OAS and TNB as substrates. The kinetic parameters obtained by fitting the dependence of the initial velocities on the substrate concentration to Equation 11 are reported in Table III. The $Trp^{50} \rightarrow$ Tyr mutation has no effect on either the catalytic rate of the reaction or the affinity of the enzyme for the first substrate, OAS, whereas the K_m for TNB decreases by 2.7-fold. The $Trp^{161} \rightarrow$ Tyr mutation causes a 2-fold increase in V_{max}, K_{OAS}, and k_{cat}/K_{TNB}.

Denaturation of W50Y and W161Y Mutants Monitored by Circular Dichroism—The dependence on guanidinium hydrochloride concentration of the mean residue ellipticity at 222 nm of WT holo-OASS and of single tryptophan mutants is shown in Fig. 4. The W161Y denaturation curve is completely superimposable with that of the WT enzyme, indicating that the mutation has not altered the susceptibility of the secondary structure to denaturation. The thermodynamic parameters, obtained as indicated under "Experimental Procedures," are listed in Table IV. $\Delta G^0_{0,U}$ and D_{50} are identical, within the experimental error, to those of the WT protein, indicating that the global stability of the enzyme is not sensitive to the mutation of Trp^{161}. The behavior of the W50Y mutant is strikingly different from that of the WT enzyme and the W161Y mutant. The denaturation curve is significantly shifted toward lower GdnHCl concentrations, with a D_{50} of about 0.3 M, indicating that the mutation of Trp^{50} has dramatic effects on the protein global stability.

Denaturation of W50Y and W161Y Mutants Monitored by Fluorescence Emission upon Excitation at 298 nm—Due to the presence of a single tryptophan residue in each of the two domains of WT OASS, the fluorescence emission upon excitation at 298 nm is a sensitive probe of structural changes in either the N- or C-terminal domain, thus allowing a characterization of the differences in their stability and the effects of the mutation on local dynamics. The tryptophan residues of W50Y and W161Y mutants are both involved in an energy transfer process to the cofactor (Fig. 3). The fluorescence emission intensity of tryptophan depends on both local changes in tryptophan environment and the distance and orientation of the aromatic residue with respect to PLP. The dependence of the fluorescence emission intensity on GdnHCl concentration is shown in Fig. 5. The unfolding transition of W161Y mutant is qualitatively similar to that of the WT enzyme, implying that the mutation has not altered the unfolding mechanism of OASS. The thermodynamic parameters for the unfolding of the W161Y mutant are shown in Table V. The $Trp^{50} \rightarrow$ Tyr mutation deeply affects the unfolding behavior of OASS, which shows two distinct phases. The first phase, between 0 and 0.8 M GdnHCl, is characterized by an increase in the fluorescence intensity. In the second phase, from 0.8 to about 1.5 M GdnHCl, the fluorescence intensity decreases. The transition midpoints for the W50Y mutant denaturation (0.5 and 1.0 M) are both left-shifted with respect to the transition midpoint of the WT enzyme.

Quenching of the Cofactor Fluorescence Emission by Acrylamide—The Stern-Volmer plots of the quenching by acrylamide of PLP fluorescence emission for the W161Y mutant and both the open and closed forms of the WT enzyme are presented in Fig. 6. The dependence of F_0/F on quencher concentration does not follow a simple linear relationship as is commonly observed for dynamic quenching of a homogenous mixture of equivalent fluorophores. A downward curvature of the Stern-Volmer plot is commonly considered the mark of a heterogeneous ensemble of two noninteracting fluorophores, one of which is inaccessible to the quencher (29). By fitting the curve to Equation 1, two parameters are obtained: K^A_{SV}, the Stern-Volmer constant for the quenching of the accessible site, and f_A, the fraction of initial fluorescence (*e.g.* in the absence of quencher) emitted by the accessible species. The fitting of the

TABLE I
Fluorescence lifetimes and fractional intensities for WT OASS, W50Y mutant, and W161Y mutant

OASS	τ_1	τ_2	τ_3	f_1	f_2	f_3
	ns	*ns*	*ns*			
WT	5.5 (Trp^{50})[a]	2.1 (Trp^{161})[a]	0.7	0.055	0.724	0.222
W50Y		2.3	0.8		0.914	0.086
W161Y	4.7		0.9	0.251		0.749

[a] Predominant contribution (7).

TABLE II
Secondary structure content of WT holo-OASS, W50Y mutant, and W161Y mutant

Circular dichroism spectra were collected on a solution containing 3 μM OASS, 20 mM phosphate buffer, pH 7.0, at 20 °C. Values were obtained from the deconvolution of the far-UV CD spectra using the CD Spectra Deconvolution software, version 2.1 (28).

OASS	α-Helix	β-Sheets	Other
	%	%	%
WT	37.0	14.0	45.6
W50Y	35.6	15.2	46.0
W161Y	34.1	16.3	48.2

TABLE III
Kinetic parameters for the reaction catalyzed by OASS using OAS and TNB as substrates, 100 mM Hepes, pH 7.0, at 20 °C

The initial velocity was measured as a function of OAS concentration at different concentrations of TNB. The enzyme concentration was 25 μg/ml. OAS and TNB concentrations were varied over the range 0.5–2 mM and 25–100 μM, respectively.

	OASS WT	OASS W50Y	OASS W161Y
V_{max} (μM/min)	0.4 ± 0.1	0.4 ± 0.1	0.9 ± 0.1
V_{max}/E_t (min^{-1})	0.54 ± 0.13	0.56 ± 0.15	1.25 ± 0.15
K_{OAS} (μM)	749 ± 195	774 ± 113	1771 ± 302
k_{cat}/K_{OAS} (M^{-1} s^{-1})	12 ± 4	12 ± 4	12 ± 2
K_{TNB} (μM)	49 ± 12	18 ± 4	61 ± 13
k_{cat}/K_{TNB} (M^{-1} s^{-1})	184 ± 63	519 ± 180	341 ± 83

Stern-Volmer plot of WT OASS in the open conformation gives a value for the Stern-Volmer constant of 34 M^{-1} and a fraction of accessible fluorophore of 0.92. The Stern-Volmer constant decreases to a value of 21 M^{-1} for the W161Y mutant, indicating a reduced accessibility of the fluorophore with respect to the WT enzyme. The Stern-Volmer plot of the W161Y mutant lies between that of the WT protein in the open conformation and that of the WT OASS in the closed conformation, which shows a K^A_{SV} of 13 M^{-1}.

DISCUSSION

Alignment of 62 sequences of OASS from eucaryotes and procaryotes allowed us to establish that Trp^{50} is conserved only among 16% of the sequences analyzed, whereas Trp^{161} is highly conserved among eucaryotes and procaryotes (63% of the sequences). Position 50 can be occupied by a large variety of amino acids differing for polarity, molecular mass, and charge. In contrast, position 161 is occupied by a tryptophan residue in all 15 analyzed eucaryotic sequences. In procaryotes, position 161 tolerates only large apolar amino acids. Tyr residues are present, for both positions, in only one of 62 sequences analyzed.

Effects of Tryptophan Substitutions on the Secondary Structure and Tryptophan Microenvironment of OASS—The impact of Trp to Tyr substitutions on the protein secondary structure is negligible, as would be expected from a mutation of surface residues. The small differences found between the circular dichroism spectra obtained for the two mutants and that of the wild type protein can be ascribed to the contribution of tryptophan residues to the far-UV spectrum (45). In fact, the relative content of secondary structure elements is not significantly different from that of the wild type protein (Table II). Fluorescence emission spectra of the two mutants (Fig. 3) are qualitatively similar to that of the wild type protein, showing two peaks at 330 and 500 nm. In the wild type protein, the emission at 500 nm, attributed to an energy transfer process between tryptophan and PLP, arises mainly from the contribution of the Trp^{50} emission, which is transferred with high efficiency to the cofactor (8, 46). As a consequence, the tryptophan emission band of the wild type protein, centered at around 330 nm, is mainly attributable to the contribution of Trp^{161}. In the emission spectrum of the W161Y mutant, a finite emission at 330 nm is present, indicating that some of the excitation energy is directly emitted from Trp^{50}. The emission spectrum of the W50Y mutant indicates the presence of some structural perturbations affecting the emission properties of the fluorophore. In fact, the sum of the emission spectra of the two single tryptophan mutants (Fig. 3) does not coincide with the emission spectrum of the wild type protein. The mutation of Trp^{50} to

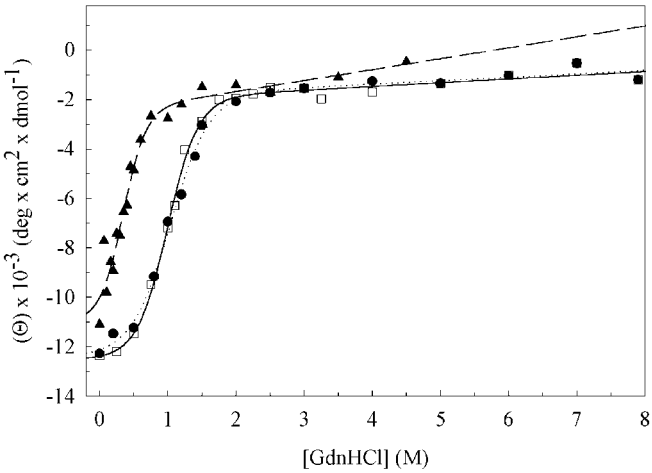

FIG. 4. **Dependence on denaturant concentration of the mean residue ellipticity at 222 of WT holo-OASS, W50Y mutant, and W161Y mutant.** Solutions of the W161Y mutant (*open squares*), W50Y mutant (*closed triangles*), and WT OASS (*closed circles*) at a protomer concentration of about 3 μM were incubated for 24 h at 20 °C in the presence of different GdnHCl concentrations. Far-UV circular dichroism spectra were collected at 20 °C, and the mean residue ellipticity at 222 nm was plotted as a function of GdnHCl concentration. The *lines* represent the fitting of the data to a two-state model according to Equation 2. Thermodynamic parameters are given in Table IV.

TABLE IV
Thermodynamic parameters for the denaturation of WT OASS and OASS W161Y obtained from circular dichroism spectra

OASS	$\Delta G^0_{0,U}$	D_{50}	m
	kcal/mol	*M*	*kcal* × *M/mol*
W161Y	2.57 ± 0.12	0.99 ± 0.06	2.60 ± 0.11
WT	2.27 ± 0.16	1.04 ± 0.09	2.22 ± 0.14

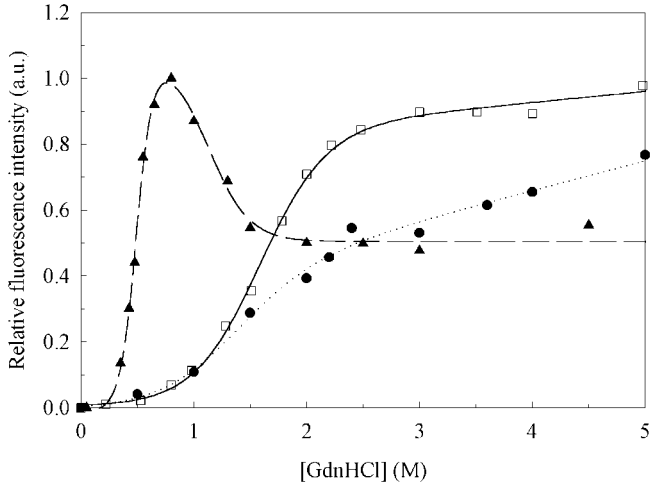

FIG. 5. **Dependence on denaturant concentration of the fluorescence emission intensity of WT holo-OASS, W50Y mutant, and W161Y mutant.** Solutions containing 6 μM W161Y mutant (*open squares*), W50Y mutant (*closed triangles*), and WT OASS (*closed circles*) were incubated for 24 h at 20 °C in the presence of different GdnHCl concentrations. Fluorescence emission spectra upon excitation at 298 nm were recorded at 20 °C. The emission intensity at the indicated wavelengths is reported as a function of the denaturant concentration. The *lines* represent the fitting of the data to a two-state model according to Equation 1. Thermodynamic parameters are given in Table V.

TABLE V
Thermodynamic parameters for the denaturation of WT OASS and OASS W161Y obtained from fluorescence emission spectra upon excitation at 298 nm

OASS	$\Delta G^0_{0,U}$	D_{50}	m
	kcal/mol	*M*	*kcal* × *M/mol*
W161Y	3.05 ± 0.09	1.55 ± 0.07	1.97 ± 0.06
WT	2.72 ± 0.36	1.39 ± 0.26	1.96 ± 0.26

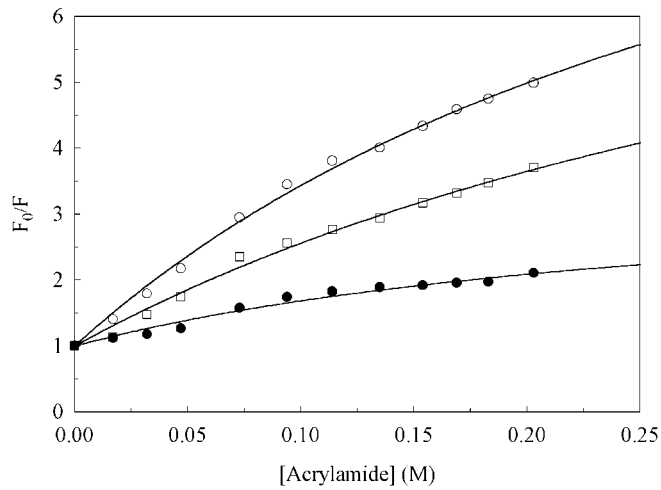

FIG. 6. **Stern-Volmer plots of quenching by acrylamide of pyridoxal phosphate fluorescence emission for WT OASS and W161Y mutant.** Quenching of cofactor fluorescence was measured on solutions containing 40 μM OASS protomers as a function of acrylamide concentration. Experiments on the open form of the WT and W161Y OASS were performed in 100 mM Hepes, pH 7.0, whereas experiments on the closed form of the WT protein were performed in 100 mM Ches, pH 9.0, in the presence of 100 mM L-Ser. Spectra were recorded upon excitation at 330 nm. The fitting to Equation 1 (*solid lines*) of the emission intensity at 394 nm for WT OASS open form (*open circles*), at 405 nm for WT OASS closed form (*closed circles*), and at 389 nm for W161Y mutant (*open squares*), gave the following Stern-Volmer constants: 34, 13, and 21 M^{-1} for WT OASS in the open and closed conformation and W161Y mutant, respectively.

Tyr is responsible for an increase in the energy transfer efficiency between Trp^{161} and PLP with respect to the wild type protein. Alterations of the emission spectrum of the protein might be a consequence of a reorientation of the cofactor with respect to the tryptophan residue. The Schiff base lysine, Lys^{41}, and Trp^{50} are both placed on helix 1 in the N-terminal domain. In the wild type OASS, Trp^{50} is involved in the formation of a hydrogen bond with Ser^8. The different dimensions and spatial orientation of tyrosine with respect to tryptophan are likely to generate repulsive interactions with Ser^8 or with other neighboring residues that might be minimized at the expense of small rearrangements in the position of helix 1. The effect of the rearrangement of helix 1, not appreciable in circular dichroism spectroscopy, on the mutual orientation of PLP and Trp^{161} is reflected in an increase in energy transfer efficiency between the two residues. Moreover, one has to take into account the possibility that some energy transfer occurs, in the wild type protein, from Trp^{161} to Trp^{50}. In this case, the missing competition between Trp^{50} and PLP in the W50Y mutant could give a minor contribution to the observed spectral behavior.

Effects of the Mutations on the Active Site Structure, Function, and Accessibility—The two mutants both retain the capacity of binding pyridoxal 5′-phosphate, as demonstrated by the visible absorbance spectra (Fig. 2) that are characterized by a peak at 412 nm, typical of the ketoenamine tautomer of the internal aldimine formed between PLP and Lys^{41} (41). Studies of the wild type protein demonstrated that the affinity of the cofactor for the unfolded enzyme is very low (6) and that PLP binds with high affinity to the apo form of the enzyme to give a fully functional holo-OASS (47). These data suggest that PLP binding is a late event in the folding process of OASS and takes place on an already structured active site. Since the ability to bind PLP is highly dependent on the presence of a correctly folded active site, the unperturbed binding of the cofactor to the two mutants indicates that the substitutions do not significantly affect the structure of the apoenzyme active site. Accordingly, the W50Y mutant shows an absorption spectrum that is superimposable with that of the wild type protein. On the other hand, the visible spectrum of the W161Y mutant shows a small but significant increase in the absorption around 320 nm, suggesting the presence of a higher content of the enolimine tautomer of the cofactor (43). The stabilization of the enolimine tautomer of the internal aldimine, which is favored in apolar environments (43), indicates that the Trp^{161} to Tyr mutation might have induced slight alterations in active site environment. An alteration in the active site environment is confirmed by fluorescence quenching data (Fig. 6). The Stern-Volmer constant obtained for the quenching of PLP in the W161Y mutant (K^A_{SV} = 21 M^{-1}) is significantly lower than that of the WT protein in the open conformation (K^A_{SV} = 34 M^{-1}), indicating a reduced accessibility to the fluorophore that resides in the cleft between the N-terminal and the C-terminal domain. The effect is less pronounced than that observed for the WT protein in the closed conformation (K^A_{SV} = 13 M^{-1}) and suggests that the mutation of Trp^{161} may have induced a partial closure of the active site. Stern-Volmer plots, differently from those obtained in similar experiments on tryptophan synthase (48), show a downward curvature. This behavior is consistent with the presence of two noninteracting fluorophores, one of which is not quenched (29). Such behavior could arise from a fraction of protein molecules in a tightly closed conformation that makes the active site totally inaccessible to the quencher or from the presence of a nonquenchable, although accessible, isomer of the coenzyme.

The effects of the mutations on the enzymatic activity are

different for the two single tryptophan mutants (Table III). Since the k_{cat}/K_{OAS} does not change compared with the wild type enzyme for any of the mutant enzymes, either the mutations do not affect the first half of the reaction, or the effects are compensatory. The W50Y mutant exhibits a 3-fold increase in k_{cat}/K_{TNB} and a 3-fold decrease in K_{TNB}. The effect can thus be attributed to K_{TNB} and is probably an effect on a rate process not included in k_{cat} (*i.e.* a rate constant contained in K_{TNB}, k_7, or k_8 (see Equations 8 and 10)). It is possible that k_7 could be increased as the orientation of the aminoacrylate Schiff base changes slightly as suggested to explain the more efficient energy transfer in the W50Y mutant enzyme or that the conformational change that occurs upon diffusion of TNB into the active site is more efficient, giving a decrease in the off-rate constant for TNB from the *E*(AA)TNB complex.

Mutation of Trp^{161} to Tyr gives ~2-fold increases in V_{max}, k_{cat}/K_{TNB}, and K_{OAS} (Table III). Since k_{cat}/K_{OAS} is unchanged, the effect must be on a rate process in the second half of the reaction. It is likely that the chemistry is rate-determining in the second half of the reaction using TNB as substrate, and the release of product is fast compared with the addition/elimination steps. Thus, with $k_{11} > k_3$, k_{10} the expressions for K_{OAS}, k_{cat}, and k_{cat}/K_{TNB} are as follows,

$$\frac{V}{E_t} = \frac{k_3 k_9}{k_3 + k_9} \quad \text{(Eq. 12)}$$

$$\frac{V}{K_{TNB} E_t} = \frac{k_7 k_9}{k_8 + k_9} \quad \text{(Eq. 13)}$$

$$K_{OAS} = K_d \left[\frac{1 + \frac{k_3}{k_2}}{1 + \frac{k_3}{k_9}} \right] \quad \text{(Eq. 14)}$$

and an increase in k_9 will result in an increase in all three parameters as long as k_9 is of the same magnitude as k_3, k_8, and k_2.

As can be observed in the crystal structure, Trp^{50} and Trp^{161} are not directly involved in the processes taking place in the active site, such as the anchorage of the cofactor to the protein matrix (8), the binding of the substrate (4), and catalysis (8). Therefore, the effects observed on the enzymatic activity must be a consequence of conformational changes in the active site or in regulatory regions of the protein once the α-aminoacrylate Schiff base has been formed, induced by structural rearrangements associated to the mutations. In the case of W161Y mutant enzyme, these effects could be the result of a more efficient trapping of the nucleophilic substrate as it diffuses into the active site.

Unfolding Behavior of the W50Y Mutant—The dependence on the denaturant concentration of the mean residue ellipticity at 222 nm of the W50Y mutant (Fig. 4) is shifted to lower denaturant concentrations with respect to the wild type protein and shows a greater post-transition slope. Due to the fact that the denaturation of the W50Y mutant is not fully reversible, it is not possible to calculate significant thermodynamic parameters from the denaturation curves. The shift in the transition midpoint is suggestive of a destabilization of the protein structure, although it could also result from an increase of the value of parameter *m* without any effect on the unfolding free energy. The unfolding of the WT OASS was shown to be an apparently two-state reaction (6), with the monomerization process taking place on a partially unfolded protein. For this reason, the unfolding curves of WT OASS do not show any protein concentration dependence, and monomeric intermediates do not accumulate during the denaturation of the enzyme. In contrast, the unfolding curves of the W50Y mutant enzyme, monitored by

FIG. 7. **Three-dimensional structure of a WT OASS subunit.** The mobile subdomain of the N-terminal domain (*blue*), the loop spanning residues 140–146 (*orange*), the two helices carrying Trp^{50} (*red*) and Trp^{161} (*green*), and the cofactor (*yellow*) are shown.

circular dichroism, show a dependence on the protein concentration between 0 and 0.8 M GdnHCl (data not shown), indicating a monomerization process taking place concomitantly with the unfolding. Therefore, the mutation of Trp^{50} to Tyr induces a dramatic change in the unfolding mechanism, leading to the coupling of protein denaturation and subunit dissociation. Furthermore, the unfolding curve of the W50Y mutant enzyme (Fig. 5) shows a fluorescence intensity maximum around 0.8–1 M GdnHCl, which is not present for the wild type protein. As recently pointed out (49), the assignment of hyperfluorescent maxima during protein unfolding to denaturation intermediates should be done cautiously. In fact, although hyperfluorescent maxima may correspond to unfolding intermediates, hyperfluorescence could also derive from the increased pretransition flexibility of native states that possess quenched fluorophores. In the W50Y mutant enzyme, Trp^{161} fluorescence, differently from the wild type protein, is partially quenched by PLP and during unfolding the increase of the flexibility of the native state could result in the appearance of hyperfluorescence not directly related to the stabilization of an unfolding intermediate. The range of GdnHCl concentrations associated with the appearance of hyperfluorescence does correspond to the range in which the monomerization takes place. This result indicates the presence of an unfolding intermediate deriving from the reorganization of a partially unfolded monomeric species. The detailed unfolding mechanism and the nature of the intermediate will be addressed elsewhere.[2] However, the unfolding behavior of the W50Y mutant is a remarkable example of the deep perturbation of protein stability and/or unfolding mechanism caused by the substitution of a single, nonconserved residue. The mutation does not perturb the native state of the protein, as indicated by the conservation of the protein secondary structure, the fluorescence lifetimes, and the quaternary organization, as indicated by fluorescence anisotropy data (data not shown). The specific structural role played by Trp^{50} was previously pointed out by the observation

[2] B. Campanini, S. Raboni, S. Vaccari, L. Zhang, P. F. Cook, T. L. Hazlett, A. Mozzarelli, and S. Bettati, manuscript in preparation.

that the substitution of Trp^{50} with Phe led to very low protein expression and recovery after purification.[3] Overall, the data indicate that the N-terminal domain is endowed with a marginal stability, as previously suggested by fluorescence lifetime studies on the wild type protein (7). The low stability of the N-terminal domain, necessary for the structural plasticity required for the catalytic function, is maintained by a delicate balance between stabilizing and destabilizing interactions and is thus susceptible to significant perturbations in response to small changes of the amino acid sequence. The changes observed in the catalytic activity induced by the W50Y mutation are probably associated with the destabilization of the native structure and with alterations of the conformational flexibility of the N-terminal domain.

Denaturation and Stability of the W161Y Mutant—The mutation of Trp^{161} to Tyr does not cause significant effects on the protein unfolding mechanism, as shown by the overlapping between the unfolding curves obtained in circular dichroism for the W161Y mutant and the wild type protein (Fig. 4). The thermodynamic parameters correspond to those obtained for the wild type protein (Table IV) (6) and indicate that the mutation does not influence the protein secondary structure stability. The conservation of Trp^{161} among sequences from different organisms is, thus, not required for structural stabilization and must have originated from different evolutionary pressures. The dependence of the fluorescence emission intensity on denaturant concentration is also nearly superimposable with that obtained for the wild type protein (Fig. 5 and Table V). Fluorescence emission allows the detection of the events taking place within the N-terminal domain. The dependence of the fluorescence emission intensity on denaturant concentration for the WT protein is sensitive to the unfolding dynamics of both the N- and C-terminal domain and to their relative stability. The correspondence between the stabilization free energies calculated for the wild type protein and those calculated for the N-terminal domain on the W161Y mutant (Table V) provides a strong indication of a stabilizing effect on the N-terminal domain exerted by the amino acid substitution in the C-terminal domain. Furthermore, the D_{50} value for the unfolding of the N-terminal domain, as calculated from fluorescence lifetime experiments (7), is 0.75 ± 0.03 M, whereas in the W161Y mutant it is shifted to 1.55 ± 0.07 M.

The effects of a point mutation can be transmitted to different regions of the protein both through direct interactions of residues that are separated in the primary sequence but are in contact in the three-dimensional structure and indirectly through conformational changes such as those that allow allosteric regulation. Trp^{161} makes no direct interactions with the N-terminal domain, since all of its contacts are established with residues of helix 6 and 7 and with loops of the C-terminal domain (residue contacts were derived with the CSU software; see Ref. 50). Helix 6, which contains Trp^{161}, is connected by a short loop of seven residues (amino acids 140–146) (Fig. 7) to the N-terminal domain and, in particular, to the subdomain (residues 87–131) that rotates upon substrate binding, which leads to the open to closed transition. The transition, which allows for orientation preceding catalysis and the shielding of reactive catalytic intermediates from the solvent, is a fundamental step in the control of the progression of the enzymatic activity. The dynamic quenching of PLP emission by acrylamide is significantly reduced in the W161Y mutant enzyme with respect to the WT protein. However, the accessibility of the fluorophore of the W161Y mutant enzyme is still higher than that of the closed form of the WT protein, in which the cofactor is almost completely shielded from the solvent. Therefore, the single point mutation is related to long range effects involving the structural elements regulating the accessibility of the cofactor and the dynamics associated to the trapping of the nucleophilic substrate. As recently pointed out by theoretical studies on protein structures (51), the increase in structural stability associated, for example, with amino acid mutations of protein regions that are involved in conformational changes triggered by substrate binding, results in a decrease in the affinity of the substrate for the protein. The increase of K_m for OAS observed in the W161Y mutant of holo-OASS is small if compared with the effect of mutations affecting directly the active site structure and/or stability, but its magnitude is comparable with that induced on OASS by the interaction with serine acetyltransferase (SAT) (52–54). SAT catalyzes the synthesis of *O*-acetyl-L-serine (55) and in the cell forms a bienzymatic complex with OASS, called cysteine synthase. The formation of the complex has opposite effects on the activity of the two enzymes: the K_m of L-serine and acetyl-CoA for SAT decreases, whereas the K_m of OAS and sulfide for OASS increases (52, 53). The biological significance of this regulation remains unclear as the structural mechanism of the interaction of SAT with OASS. The effects of the substitution of Trp^{161} with a tyrosine on the protein dynamics, activity, and structural stability, together with the unusual exposure of Trp^{161} to the solvent (Fig. 1), its location in a flat surface of the protein, and its high degree of conservation, suggest a possible role of this residue in the regulation pathway of OASS activity by SAT. The regulation could occur through an allosterically controlled open to closed transition triggered by the association with SAT. More studies are needed to further confirm this hypothesis, and experiments on the effect of the interaction between SAT and the W161Y mutant are currently under way.

Acknowledgments—We gratefully acknowledge Professor Gian Luigi Rossi (Department of Biochemistry and Molecular Biology, University of Parma) and Dr. Enrico Gratton (Laboratory of Fluorescence Dynamics, University of Illinois) for helpful discussion. We thank Dr. Roberto Silva (Department of Genetics, University of Parma) for valuable assistance with cellular cultures. Circular dichroism experiments were performed at the Centro Interdipartimentale Misure of the University of Parma.

REFERENCES

1. Kuske, C. R., Hill, K. K., Guzman, E., and Jackson, P. J. (1996) *Plant Physiol.* **112,** 659–667
2. Tai, C. H., Nalabolu, S. R., Jacobson, T. M., Minter, D. E., and Cook, P. F. (1993) *Biochemistry* **32,** 6433–6442
3. Cook, P. F., and Wedding, R. T. (1976) *J. Biol. Chem.* **251,** 2023–2029
4. Burkhard, P., Tai, C. H., Ristroph, C. M., Cook, P. F., and Jansonius, J. N. (1999) *J. Mol. Biol.* **291,** 941–953
5. McClure, G. D., and Cook, P. F. (1994) *Biochemistry* **33,** 1674–1683
6. Bettati, S., Benci, S., Campanini, B., Raboni, S., Chirico, G., Beretta, S., Schnackerz, K. D., Hazlett, T. L., Gratton, E., and Mozzarelli, A. (2000) *J. Biol. Chem.* **275,** 40244–40251
7. Bettati, S., Campanini, B., Vaccari, S., Mozzarelli, A., Schianchi, G., Hazlett, T. L., Gratton, E., and Benci, S. (2002) *Biochim. Biophys. Acta* **1596,** 47–54
8. Burkhard, P., Rao, G. S. J., Hohenester, E., Schnackerz, K. D., Cook, P. F., and Jansonius, J. N. (1998) *J. Mol. Biol.* **283,** 121–133
9. Uchiyama, T., Katouno, F., Nikaidou, N., Nonaka, T., Sugiyama, J., and Watanabe, T. (2001) *J. Biol. Chem.* **276,** 41343–41349
10. Greene, L. H., Chrysina, E. D., Irons, L. I., Papageorgiou, A. C., Acharya, K. R., and Brew, K. (2001) *Protein Sci.* **10,** 2301–2316
11. Hillier, B. J., Rodriguez, H. M., and Gregoret, L. M. (1998) *Fold Des.* **3,** 87–93
12. Eason, D. D., Shepherd, A. T., and Blanck, G. (1999) *Biochim. Biophys. Acta* **1446,** 140–144
13. Bray, M. R., Johnson, P. E., Gilkes, N. R., McIntosh, L. P., Kilburn, D. G., and Warren, R. A. (1996) *Protein Sci.* **5,** 2311–2318
14. Fulton, K. F., Jackson, S. E., and Buckle, A. M. (2003) *Biochemistry* **42,** 2364–2372
15. Marie, G., Serani, L., Laprevote, O., Cahuzac, B., Guittet, E., and Felenbok, B. (2001) *Protein Sci.* **10,** 99–107
16. Zargarian, L., Le Tilly, V., Jamin, N., Chaffotte, A., Gabrielsen, O. S., Toma, F., and Alpert, B. (1999) *Biochemistry* **38,** 1921–1929
17. Subramaniam, V., Jovin, T. M., and Rivera-Pomar, R. V. (2001) *J. Biol. Chem.* **276,** 21506–21511
18. Davidson, W. S., Arnvig-McGuire, K., Kennedy, A., Kosman, J., Hazlett, T. L., and Jonas, A. (1999) *Biochemistry* **38,** 14387–14395
19. Wallace, L. A., Burke, J., and Dirr, H. W. (2000) *Biochim. Biophys. Acta* **1478,**

[3] P. F. Cook, unpublished observation.

325–332
20. Freitag, S., Le Trong, I., Chilkoti, A., Klumb, L. A., Stayton, P. S., and Stenkamp, R. E. (1998) *J. Mol. Biol.* **279,** 211–221
21. Wrabl, J. O., Larson, S. A., and Hilser, V. J. (2001) *Protein Sci.* **10,** 1032–1045
22. Honda, Y., Fukamizo, T., Okajima, T., Goto, S., Boucher, I., and Brzezinski, R. (1999) *Biochim. Biophys. Acta* **1429,** 365–376
23. Watanabe, H., Kragh-Hansen, U., Tanase, S., Nakajou, K., Mitarai, M., Iwao, Y., Maruyama, T., and Otagiri, M. (2001) *Biochem. J.* **357,** 269–274
24. Tai, C. H., and Cook, P. F. (2000) *Adv. Enzymol. Relat. Areas Mol. Biol.* **74,** 185–234
25. Rege, V. D., Kredich, N. M., Tai, C. H., Karsten, W. E., Schnackerz, K. D., and Cook, P. F. (1996) *Biochemistry* **35,** 13485–13493
26. Hara, S., Payne, M. A., Schnackerz, K. D., and Cook, P. F. (1990) *Protein Expression Purif.* **1,** 70–76
27. Pace, C. N., and Scholtz, J. M. (1997) in *Protein Structure* (Creighton, T. E., ed) 2nd Ed., Oxford University Press, Oxford, UK
28. Bohm, G., Muhr, R., and Jaenicke, R. (1992) *Protein Eng.* **5,** 191–195
29. Eftink, M. R., and Ghiron, C. A. (1981) *Anal. Biochem.* **114,** 199–227
30. Spencer, R. D., and Weber, G. (1969) *Ann. N. Y. Acad. Sci.* **158,** 361–376
31. Gratton, E., and Limkeman, M. (1983) *Biophys. J.* **44,** 315–324
32. Jameson, D. M., and Hazlett, T. L. (1991) in *Biophysical and Biochemical Aspects of Fluorescence Spectroscopy* (Dewey, T. G., ed) pp. 106–133, Plenum Publishing Corp., New York
33. Beechem, J. M., and Gratton, E. (1988) in *Time-Resolved Laser Spectroscopy in Biochemistry*, SPIE Proceedings Vol. 909 (Lakowicz, J. R., ed) pp. 70–81, International Society for Optical Engineering, Bellingham, WA
34. Greene, R. F., and Pace, C. N. (1974) *J. Biol. Chem.* **249,** 5388–5393
35. Hwang, C. C., Woehl, E. U., Minter, D. E., Dunn, M. F., and Cook, P. F. (1996) *Biochemistry* **35,** 6358–6365
36. Woehl, E. U., Tai, C. H., Dunn, M. F., and Cook, P. F. (1996) *Biochemistry* **35,** 4776–4783
37. Segel, I. H. (1993) *Enzyme Kinetics: Behavior and Analysis of Rapid Equilibrium and Steady-State Enzyme Systems*, John Wiley & Sons, Inc., New York
38. Altschul, S. F., Gish, W., Miller, W., Myers, E. W., and Lipman, D. J. (1990) *J. Mol. Biol.* **215,** 403–410
39. Higgins, D. G., and Sharp, P. M. (1988) *Gene* (*Amst.*) **73,** 237–244
40. Thompson, J. D., Higgins, D. G., and Gibson, T. J. (1994) *Nucleic Acids Res.* **22,** 4673–4680
41. Becker, M. A., Kredich, N. M., and Tomkins, G. M. (1969) *J. Biol. Chem.* **244,** 2418–2427
42. Cook, P. F., Hara, S., Nalabolu, S., and Schnackerz, K. D. (1992) *Biochemistry* **31,** 2298–2303
43. Faeder, E. J., and Hammes, G. G. (1971) *Biochemistry* **10,** 1041–1045
44. Strambini, G. B., Cioni, P., and Cook, P. F. (1996) *Biochemistry* **35,** 8392–8400
45. Schmid, F. X. (1997) in *Protein Structure* (Creighton, T. E., ed) Vol. 174, pp. 261–297, IRL Press, Oxford
46. Benci, S., Bettati, S., Vaccari, S., Schianchi, G., Mozzarelli, A., and Cook, P. F. (1999) *J. Photochem. Photobiol. B* **48,** 17–26
47. Schnackerz, K. D., and Cook, P. F. (1995) *Arch. Biochem. Biophys.* **324,** 71–77
48. Lane, A. N. (1983) *Eur. J. Biochem.* **133,** 531–538
49. Ervin, J., Larios, E., Osvath, S., Schulten, K., and Gruebele, M. (2002) *Biophys. J.* **83,** 473–483
50. Sobolev, V., Sorokine, A., Prilusky, J., Abola, E. E., and Edelman, M. (1999) *Bioinformatics* **15,** 327–332
51. Luque, I., and Freire, E. (2000) *Proteins* **41,** Suppl. 4, 63–71
52. Droux, M., Ruffet, M. L., Douce, R., and Job, D. (1998) *Eur. J. Biochem.* **255,** 235–245
53. Kredich, N. M., Becker, M. A., and Tomkins, G. M. (1969) *J. Biol. Chem.* **244,** 2428–2439
54. Mino, K., Yamanoue, T., Sakiyama, T., Eisaki, N., Matsuyama, A., and Nakanishi, K. (2000) *Biosci. Biotechnol. Biochem.* **64,** 1628–1640
55. Kredich, N. M., and Tomkins, G. M. (1966) *J. Biol. Chem.* **241,** 4955–4965

Surface-exposed Tryptophan Residues Are Essential for *O*-Acetylserine Sulfhydrylase Structure, Function, and Stability

Barbara Campanini, Samanta Raboni, Simona Vaccari, Lei Zhang, Paul F. Cook, Theodore L. Hazlett, Andrea Mozzarelli and Stefano Bettati

J. Biol. Chem. 2003, 278:37511-37519.
doi: 10.1074/jbc.M305138200 originally published online June 17, 2003
